Supporting Information

Reverse construction of dominant/secondary facets in Bi$_{24}$O$_{31}$Br$_{10}$ photocatalyst for boosting electronic transfer

Ling-yun Li,[a] Yue-guang Ma,[b] Qi Li,[b] Yi-lei Li,[bc] Ying-juan Hao,[b] Xiao-jing Wang,[b] Rui-hong Liu[b] and Fa-tang Li[*ab]☐

[a]College of Environmental Science and Engineering, Hebei University of Science and Technology, Shijiazhuang 050018, China. Email: lifatang@126.com

[b]College of Science, Hebei University of Science and Technology, Shijiazhuang 050018, China

[c]Key Laboratory of Theoretical and Computational Photochemistry, Ministry of Education, College of Chemistry, Beijing Normal University, Beijing 100875, China

Experimental

Materials and methods

Tetrabutylammonium bromide ($(C_4H_9)_4NBr$, TBAB) was obtained from Aladdin Reagents Co. Ltd (Shanghai, China), and the bismuth nitrate pentahydrate ($Bi(NO_3)_3 \cdot 5H_2O$), urea ($CO(NH_2)_2$), Rhodamine B (RhB), were purchased from Sinopharm (Shanghai, China). All chemicals were of analytical grade and used without further purification.

In a typical synthesis procedure, $Bi(NO_3)_3 \cdot 5H_2O$ mixed with TBAB and urea, then the mixed was heated on an electric furnace until the formation of a white solution, which is an ionic liquid (IL, $[(C_4H_9)_4N]^+[Bi(NO_3)_3Br]^-$) . After that, the IL was transferred into a tube furnace maintained at 500 °C and heated at a heating rate of 20 °C min^{-1} with a O_2 flow rate of 800 mL min^{-1}. After that the $Bi_{24}O_{31}Br_{10}$ was obtained when the combustion process was finished accompanying the emission a lot of gas. $Bi_{24}O_{31}Br_{10}$ with different {213} / {117} heterostructured facets can be acquired by simply adjusting the ratio of TBAB and urea. The designed various ratios of {213} / {117} are listed in Table S1, which are denoted as X (X represents the peak intensity ratio of {213} to {117}).

Catalyst characterization

The crystal structure and phase purity of the products were examined by means of X-ray diffraction (XRD, D/MAX-2500, Rigaku) analysis. The morphology of the samples was revealed by a field-emission scanning electron microscopy (FE-SEM, S4800, Hitachi). High-resolution transmission electron microscopy (HRTEM, JEM-2100, JEOL) images were acquired by an electron microscope. The photoabsorption properties of as-obtained was evaluated by UV-Vis diffuse reflectance spectra (UV-Vis DRS, Evolution-200, Thermo Scientific). Time-resolved photoluminescence spectroscopy was recorded on a FS5 Fluorescence spectrometer (Edinburgh Instruments) with an excitation source at 310 nm. The surface photovoltage (SPV) was tested on a self-made device consisting of a monochromatic light source with a

light chopper and a lock-in amplifier. The periodic on/off photocurrent response measurement was carried out on a CHI 660E electrochemical workstation (shanghai, china) using a standard three electrode quartz cell under a bias of 0 V, which contains a platinum wire as counter electrode, Ag/AgCl (saturated KCl) as reference electrode and a working electrode that was prepared by the photocatalyst films deposited on clean 1.5 cm × 1.0 cm fluoride-tin oxide (FTO) glass. 0.2 mol/L Na_2SO_4 was used as the electrolyte solution. The Mott-Schottky curve were obtained to evaluate the energy band positions of the photocatalysts at a frequency of 1 kHz using a CHI 660E electrochemical workstation in the dark. With an ac amplitude of 5 mV, electrochemical impedance spectroscopy (EIS) was carried out at the open-circuit potential and recorded ever a frequency range of $0.1 - 1 \times 10^5$ Hz.

Photocatalytic activity tests

The photodegradation of RhB (50 mg/L) under visible light irradiation was selected to study the photocatalytic activity of $Bi_{24}O_{31}Br_{10}$. Firstly, 100 mg of photocatalyst was put into 100 mL of the pollutant solution under magnetically stirring in darkness for 30 min to achieve the adsorption/desorption equilibrium. Afterwards, the mixture was illuminated with a 350 W Xe lamp with a 400 nm cut-off filter as a visible light source. During the photocatalytic process, 2 mL of the suspension was taken at regular intervals, take the supernatant after centrifugation to monitor the pollutant concentrations using a Thermo Scientific Evolution 220 UV-vis spectrophotometer at their maximum absorption wavelengths. Due to the continuous evaporation of water during the irradiation (about 5 mL reduction of 100 mL in 1 h reaction), the corresponding water was added to the solution before sampling for precise absorbance measurement. To detect the active species responsible for the degradation of RhB, various scavengers, including isopropanol (IPA, 10 mmol/L, •OH scavenger [1]), 1, 4 benzoquinone (BQ, 1 mmol/L, $•O_2^-$ scavenger [2]), and ammonium oxalate monohydrate (AO, 1 mmol/L, hole scavenger [3]) were employed in the photocatalytic degradation of RhB, p-nitro blue tetrazolium chloride (NBT, 2.5×10^{-5} mol/L) was used as an indicator of $•O_2^-$ [4]; NBT has a maximum absorption wavelength of 260 nm,

while the adduct of $\cdot O_2^-$ and NBT does not. The degradation experiment of NBT was conducted as follows: after dissolving NBT in H_2O to form a 2.5×10^{-5} mol/L solution, 0.10 g of photocatalyst was put into 100 mL of the NBT solution and then irradiated under visible light. A 350 W Xe lamp equipped with a 400 nm cut-off filter served as the visible light source. At a given interval, 5 mL of the aqueous solution was sampled, centrifuged, and filtered to remove the photocatalyst powders and then measured on a Thermo Scientific Evolution 220 spectrophotometer.

DFT calculation

The first-principles calculations were executed adopting the pseudopotential plane wave method based on density functional theory (DFT) and completed by the CASTEP module package in Material Studio (MS). The Perdew-Burke-Ernzerhof (PBE) functional was used to describe the exchange and correlation effect [5]. For all the geometry optimizations, the cutoff energy was set to be 450 eV. The Monkhorst-Pack grids were set to be $5\times1\times3$ and $4\times4\times4$ for the calculations on the {117} and {213} facets of $Bi_{24}O_{31}Br_{10}$, respectively [6].

The adsorption energy of O_2 on the $Bi_{24}O_{31}Br_{10}$ surface was defined as

$$\Delta E_{ads} = E_{ads} - E_{slab} - E_{O2}$$

where E_{ads} is the electronic energy of O_2 adsorption on the $Bi_{24}O_{31}Br_{10}$ surface, E_{slab} is the electronic energy of the clean cluster, and E_{O2} is the electronic energy of gaseous oxygen molecule. Under this definition, a more negative value indicates a stronger binding configuration.

Table S1. Designed sample compositions of different amounts from raw materials

Sample	Bi(NO$_3$)$_3$ （mol）	TBAB （mol）	Urea （mol）	Peak intensity ratio of {213} to {117}
0.64	0.01	0.0080	0.0050	0.64
0.74	0.01	0.0072	0.0088	0.74
0.83	0.01	0.0064	0.0125	0.83
1.12	0.01	0.0048	0.0200	1.12

Table S2. O$_2$ absorption energy on {213} facet

O$_2$ on {213} (eV)	{213} surface (eV)	O$_2$ gas (eV)	ΔE_{ads} (eV)
-619.46	-610.25	-9.13	-0.08

Table S3. O$_2$ absorption energy on {117} facet

O$_2$ on {117} (eV)	{117} surface (eV)	O$_2$ gas (eV)	ΔE_{ads} (eV)
-603.88	-594.80	-9.13	0.05

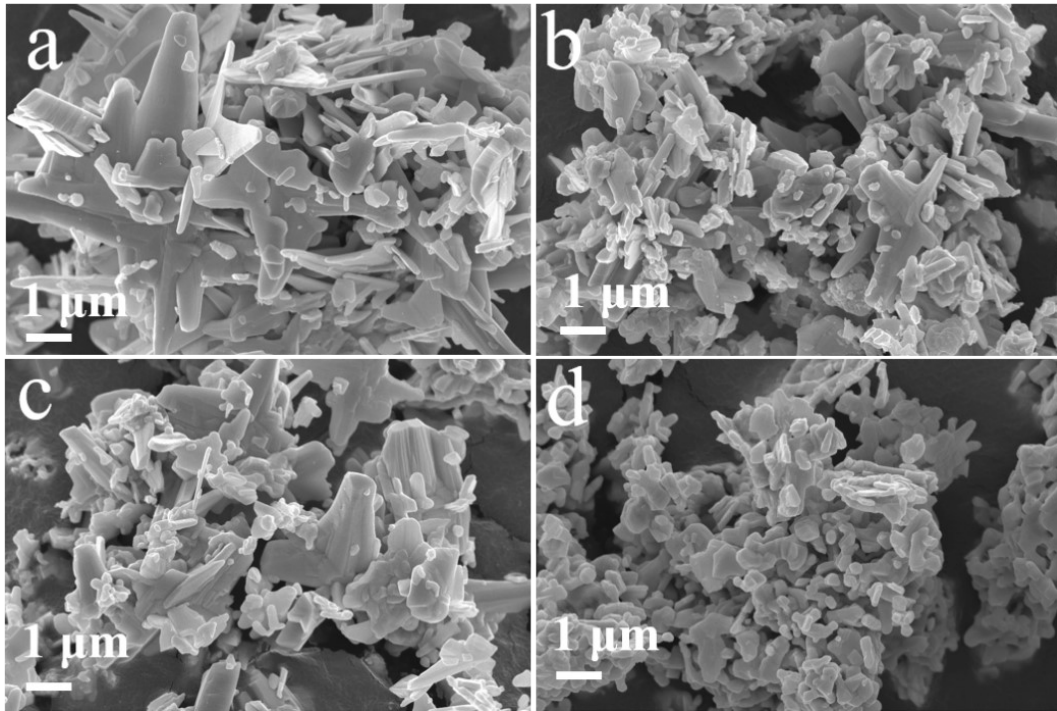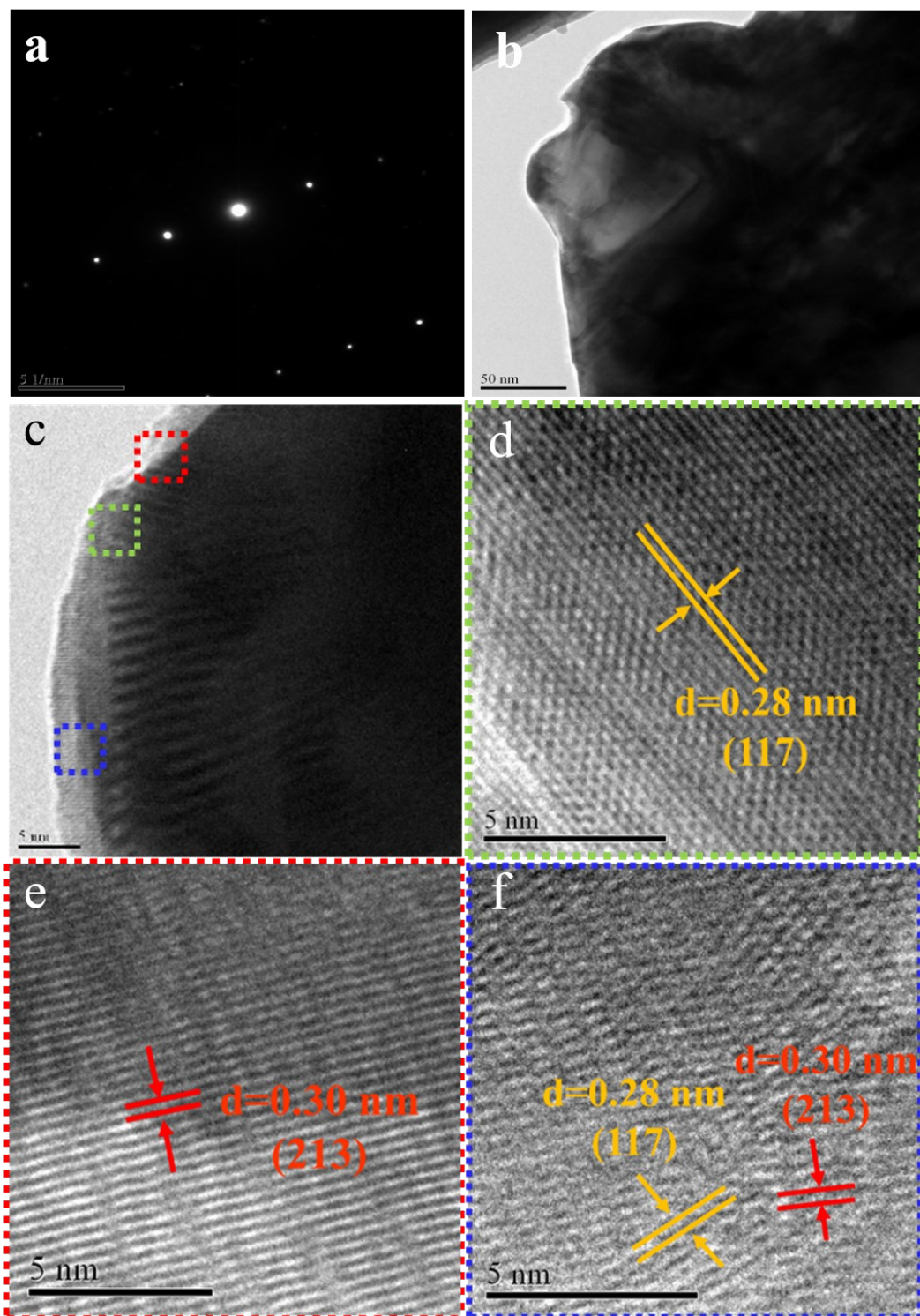**Fig. S1.** (a) (b) (c) and (d) SEM images of 0.64, 0.74, 0.83 and 1.12 $Bi_{24}O_{31}Br_{10}$, respectively.

Fig. S2. (a) Selected area electron diffraction (SAED) pattern of 0.74 $Bi_{24}O_{31}Br_{10}$, (b) and (c) TEM images of 0.74 $Bi_{24}O_{31}Br_{10}$, (d) high-resolution TEM (HRTEM) image of {117} facet of 0.74 $Bi_{24}O_{31}Br_{10}$. (e) high-resolution TEM (HRTEM) image of {213} facet of 0.74 $Bi_{24}O_{31}Br_{10}$. (f) high-resolution TEM (HRTEM) image of {213} and {117} facet-heterojunction of 0.74 $Bi_{24}O_{31}Br_{10}$.
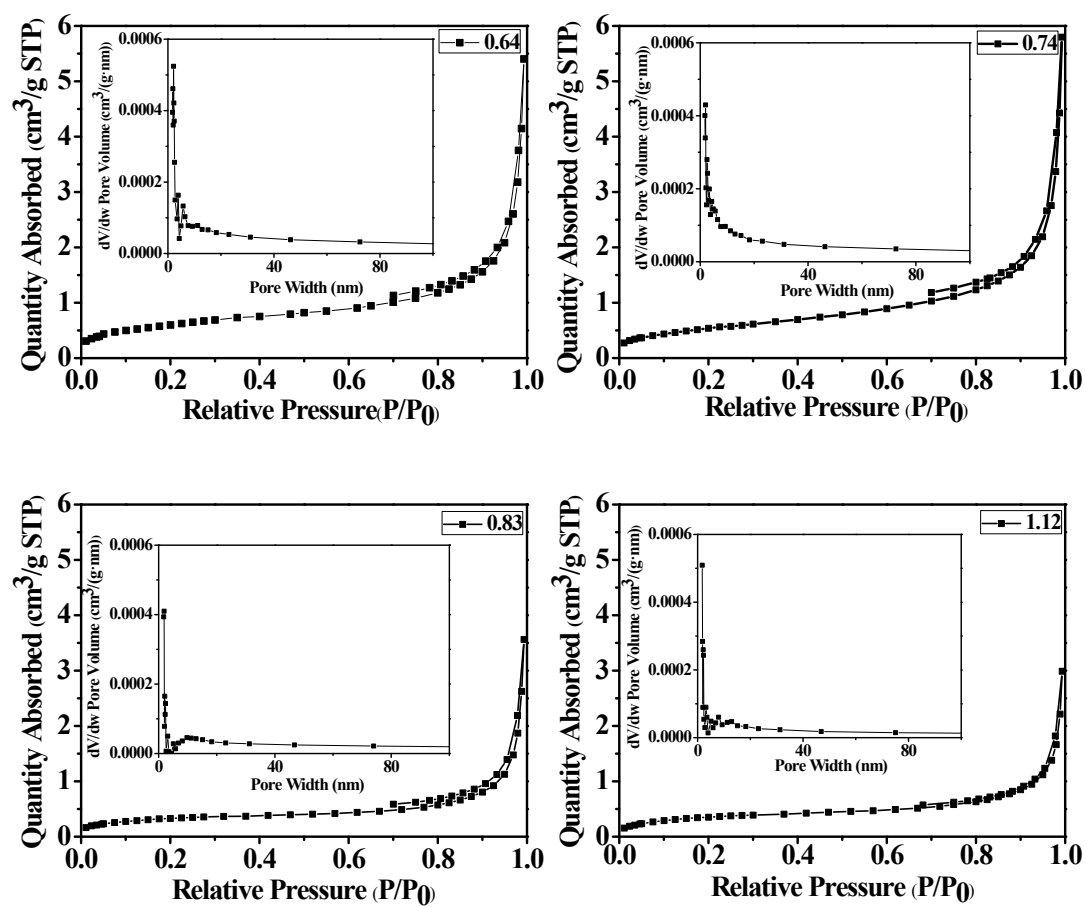
Fig. S3. Nitrogen adsorption-desorption isotherms and the corresponding pore size distribution curve (inset) for the as-synthesized samples.
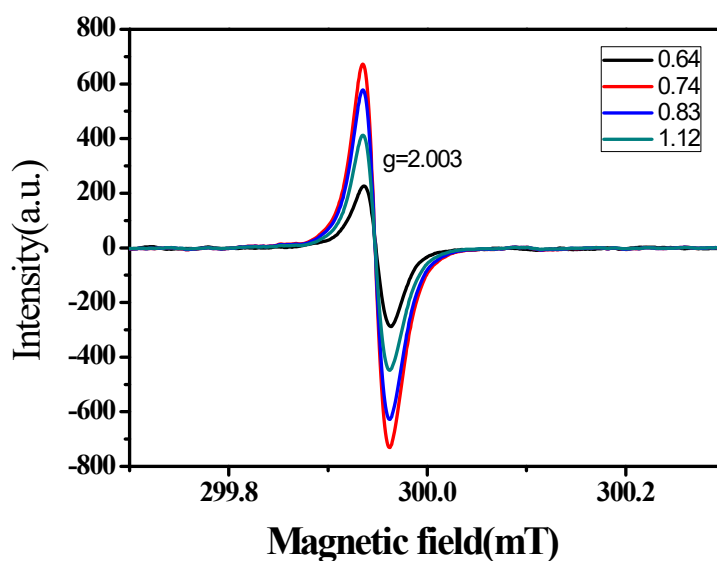
Fig. S4. ESR characterization.

In order to examine the presence of defects ESR, characterization was performed. As shown in Fig. S4, all simples have obvious signal peaks in g=2.003, which is the characteristic value of electrons trapped in oxygen vacancies (OV). However, the intensity of the peaks of simples is not consistent with their photocatalytic activity, indicating that OV do not play major role in the degradation of RhB.

Table S4. Specific surface areas and pore parameters of the as-synthesized samples.

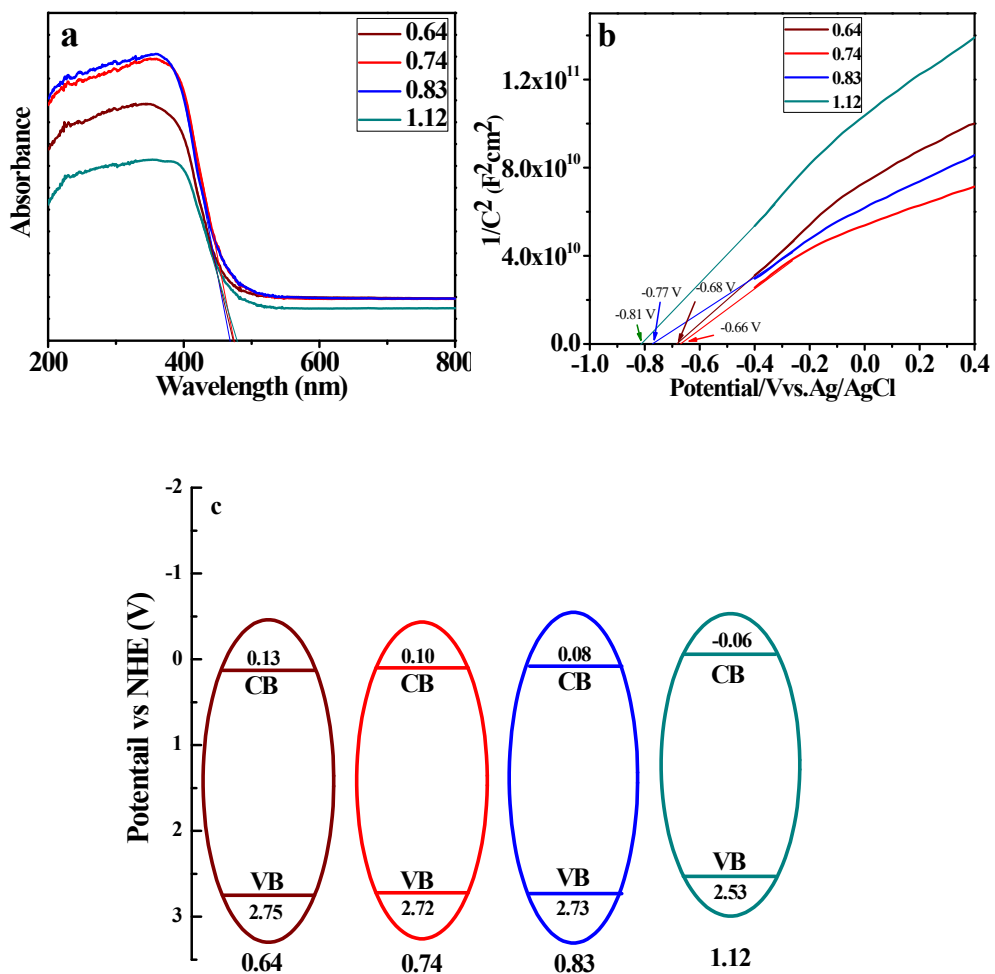| sample	S_{BET} $(m^2\ g^{-1})$	Pore volume $(cm^3\ g^{-1})$	Average pore width (nm)
0.64	2.1879	0.007293	18.1596
0.74	1.9697	0.007928	18.7882
0.83	1.1723	0.004586	26.0562
1.12	1.2805	0.003772	19.4959

Fig. S5. (a) UV–vis diffuse reflectance spectra of the as-prepared samples and (b) Mott-Schottky curves (c) Band structure
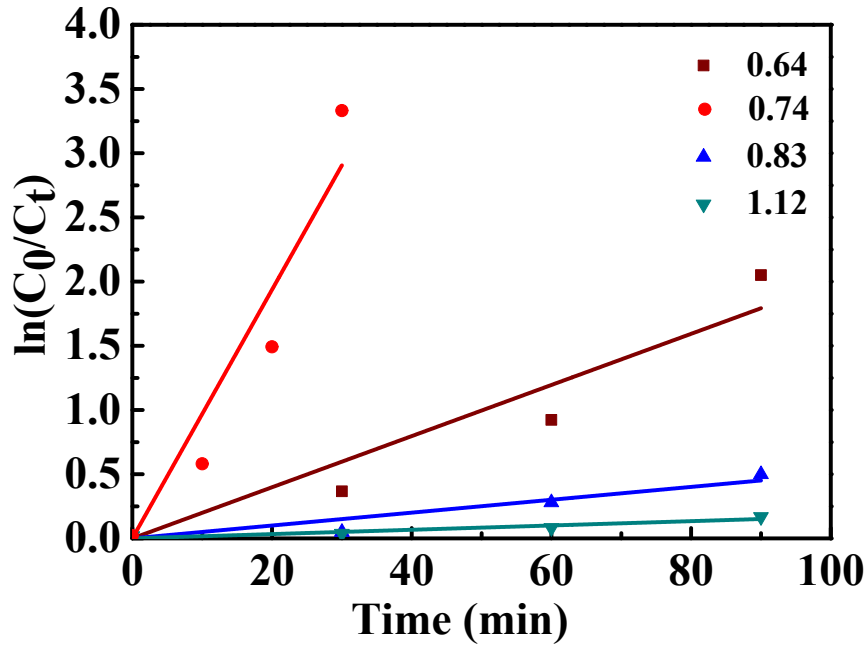
Fig. S6. First-order kinetic degradation curve

In order to quantitatively compare the photocatalytic activity of the samples, the following apparent pseudo-first-order equations is employed：

$$\ln\left(\frac{C_0}{C_t}\right) = kt + \ln\left(\frac{C_0}{C_1}\right)$$

Where k is the pseudo-first-order rate constant, C_0 is the original concentration (10 mg/L) at time -30 min, C_1 is the concentration after adsorption, and C_t is the concentration at reaction time of t. To fit the photocatalytic experiment data, the fitting curves are coerced to go through the intercepts of $\ln(C_0/C_1)$ in the yaxis, which are 0.0199, 0.0968, 0.0050 and 0.0017 for 0.64, 0.74, 0.83 and 1.12 $Bi_{24}O_{31}Br_{10}$, respectively. As shown in Fig. S6 and Table S5 that the photocatalytic activity sequence is 0.74 $Bi_{24}O_{31}Br_{10}$> 0.64 $Bi_{24}O_{31}Br_{10}$> 0.83 $Bi_{24}O_{31}Br_{10}$> 1.12 $Bi_{24}O_{31}Br_{10}$. And the reaction rate of the most active 0.74 $Bi_{24}O_{31}Br_{10}$ is nearly 60 times than that of the least active 1.12 $Bi_{24}O_{31}Br_{10}$.

Table S5. The pseudo-first order rate constants k of 0.64, 0.74, 0.83 and 1.12 $Bi_{24}O_{31}Br_{10}$

sample	Fitted equation	k (min^{-1})	Correlation coefficient (R)
0.64	$\gamma=0.0023x+0.0199$	0.0023	0.9812
0.74	$\gamma=0.0112x+0.0968$	0.0112	0.9804
0.83	$\gamma=0.0006x+0.0050$	0.0006	0.9802
1.12	$\gamma=0.0002x+0.0017$	0.0002	0.9841

Table S6. The fitted lifetimes and the corresponding percentages of 0.64, 0.74, 0.83 and 1.12 $Bi_{24}O_{31}Br_{10}$

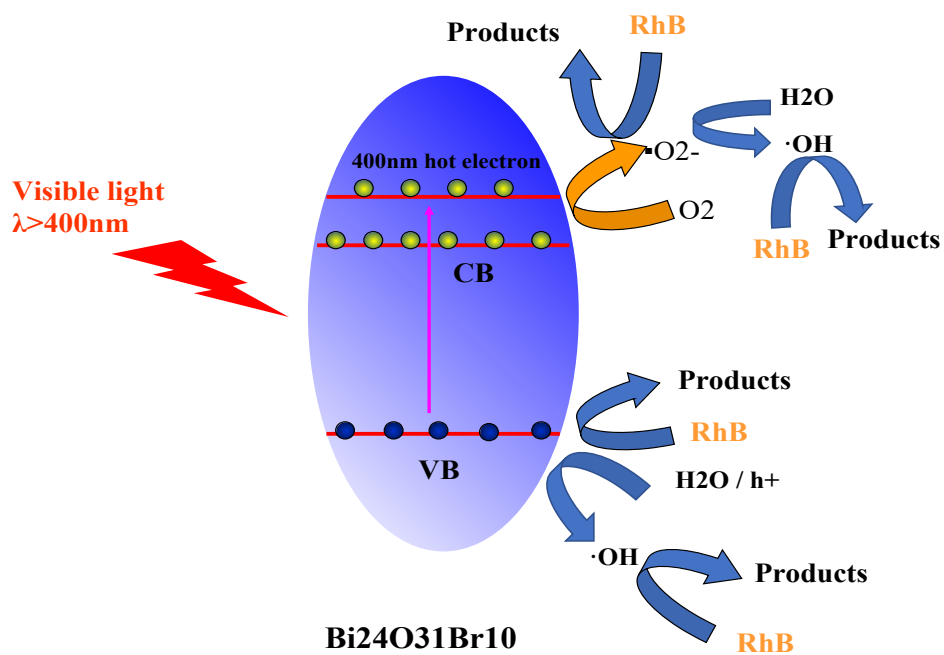| Sample	τ_1 (ns)	P_1 (%)	τ_2 (ns)	P_2 (%)	τ_3 (ns)	P_3 (%)	τ_{ave} (ns)
0.64	0.2512	66.30	1.8810	23.78	7.5712	9.92	4.81
0.74	0.2855	55.37	2.0829	31.27	9.6343	12.99	6.53
0.83	0.2211	66.68	1.8595	23.54	7.7291	9.77	4.99
1.12	0.2642	62.22	1.9408	26.75	8.5837	11.03	5.63

Fig. S7. Proposed photocatalytic degradation process

References

1. Q. Wu and Z. Zhang, *Environ. Eng. Sci.*, 2020, **37**, 109−119.
2. Q. Yi, J. Ji, B. Shen, C. Dong, J. Liu, J. Zhang and M. Xing, *Environ. Sci. Technol.*, 2019, **53**, 9725−9733.
3. R. Yuan, C. Yue, J. Qiu, F. Liu and A. Li, *Appl. Catal,. B*, 2019, **251**, 229−239.
4. B. H. Bielski, G. G. Shiue and S. Bajuk, *J. Phys. Chem.*, 1980, **84**, 830−833.
5. J. P. Perdew, K. Burke and M. Ernzerhof, *Phys. Rev. Lett.*, 1996, **77**, 3865−3868.
6. H. J. Monkhorst and J. D. Pack, *Phys. Rev. B: Condens. Matter*, 1976, **16**, 1748−1749.